# Accuracy Comparisons of Channel Emulation Methods for Two-dimensional Uniform and Three-dimensional Sectored Multi-probe Anechoic Chamber

**Xiaoyu Huang [1], Xiaoming Chen [1], Huiling Pei [1], and Yingsong Li [2,3]**

[1] School of Information and Communications Engineering
Xi'an Jiaotong University, Xi'an, 710049, China
xiaoming.chen@mail.xjtu.edu.cn

[2] College of Information and Communication Engineering
Harbin Engineering University, Harbin, 150001, China

[3] Key Laboratory of Microwave Remote Sensing
National Space Science Center, Chinese Academy of Sciences, Beijing, 100190, China

***Abstract*** ─ Multiple-input-multiple-output (MIMO) over-the-air (OTA) testing has been seen as a promising solution for evaluation of the radio performance of MIMO devices. In this work, we compare the accuracy of two channel emulation methods, i.e., the prefaded signal synthesis (PFS) and the plane wave synthesis (PWS), in two-dimensional (2D) uniform and 3D sectored multi-probe anechoic chamber (MPAC), respectively. The PWS method is proven to be more accurate than the PFS for 2D uniform MPAC system. However, for 3D sectored MPAC system, the PFS method emerged to be better than the PWS method. To explain these seemingly contradicting findings, both the required number of active probes and the leakage of power spectrum are considered in this paper. It is found that the PWS method has higher emulation accuracy than the PFS method when the number of active probes becomes sufficiently large, whereas the PFS is more robust to the undersampling due to the limited number of active probes in practical 3D sectored MPAC system. Moreover, when the number of active probes is particularly small (less than the number of clusters in the probe panel), the emulation accuracy of the PWS method outperform its counterpart.

***Index Terms*** ─Multi-probe anechoic chamber (MPAC), over-the-air (OTA), pre-faded signal synthesis (PFS), plane wave synthesis (PWS).

## I. INTRODUCTION

Multiple-input-multiple-output (MIMO) as the core technology of the new generation of mobile communication has been proposed and applied to long-term evolution (LTE), fifth generation (5G) and other wireless technologies [1]. Furthermore, with the application of millimeter wave (mm-Wave) and the reduction of antenna size, massive MIMO (M-MIMO) is widely used as a promising technology in 5G communication systems [2]-[5]. Before a MIMO device is put into use, it is important to test whether its radio performance meets the certification requirements. OTA testing has become the only feasible solution especially for mmWave M-MIMO devices. In recent years, three mainstream MIMO-OTA testing methods have been formed, including the multi-probe anechoic chamber (MPAC) method [6],[7], the reverberation chamber (RC) method [8],[9], and the radiated two-stage (RTS) method [10],[11]. The multi-probe anechoic chamber (MPAC) method, which is standardized by CTIA [12], can accurately reproduce various standard 2D radio propagation channels [13]-[15].

The main idea of the MPAC is to control the physical position and signal intensity of the probe antennas, so that the transmitted signals of multiple probes superimposed in the test area are consistent with the characteristics of the target channel [16],[17]. There are two common channel emulation methods, which are usually adopted in channel reconstruction of MPAC, i.e., the prefaded signal synthesis (PFS) and the plane wave synthesis (PWS) [18]. The basic idea of the PFS method is to reproduce the spatial characteristics of the target channel environment in the test area by controlling the power weights of the probe antennas, whereas the PWS method assigns appropriate complex weights to the probe antennas to synthesize a static plane wave field in any direction in the test area.

In this work, we make a comprehensive comparison of the emulation accuracies of the PFS and PWS techniques for both two-dimensional (2D) user equipment (UE) MIMO OTA testing and 3D massive base station (BS) OTA testing. The results show that in the traditional 2D MPAC setups, the PWS method has higher emulation accuracy than the PFS method, which is consistent with

*Submitted On: March 30, 2021*
*Accepted On: May 16, 2021*
https://doi.org/10.47037/2021.ACES.J.360903

the findings in [19]. However, when it turns to the 3D sectored MPAC system with limited active probes [20]-[22], the PFS method emerges superior performance compared to the PWS method. Then both the required number of probes and the leakage of power spectrum are considered to explain this contradicting finding. It is demonstrated that the number of active probes plays a key role in this problem. The PWS method can show superior emulation performance if there are enough required probes. In the case of limited probes, the PFS method is more accurate than the PWS method. However, when the number of probes is extremely small, the PWS method has better emulation accuracy than the PFS method again. The findings of this work not only explain contradicting finding in the literature, but also provide insight into optimal design of the 3D sectored MPAC system.

## II. METHOD

### A. Configuration of MPAC setups

Figure 1 illustrates the MPAC setup for the 2D UE OTA testing. The device under test (DUT) is located in the center of the anechoic chamber, surrounded by a horizontal ring composed of uniformly distributed probe antennas. The BS emulator generates the original test signal, which is transmitted to the channel emulator. The channel emulator simulates the multipath environment, including Doppler spread, delay spread and fast fading. Power amplifiers are necessary to compensate the path loss between the probe antennas and the DUT.

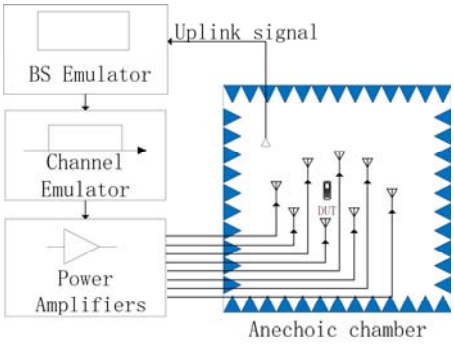


Fig. 1. Illustration of the 2D MPAC OTA setup.

Generally, the purpose of OTA testing is to accurately reproduce the power angular spectrum (PAS) of the target channel model. However, the actual PAS of the target is continuous while the emulation PAS is discrete, which is problematic to use PAS to evaluate the performance of OTA testing. The spatial correlation can be obtained from the PAS through the Fourier transform, so the spatial correlation metric can be used to evaluate the PAS indirectly [19]. In the sequel, the spatial correlation is used to evaluate the emulation performance of the PFS and PWS methods in the case of 2D UE OTA testing.

For the massive BS OTA testing, a 3D sectored MPAC setup was proposed [20], as shown in Fig. 2. The setup consists of an anechoic chamber, a DUT (i.e., a BS array), a probe panel covering a certain angle area, a switching network for selecting a specific number of active probe antennas from the probe panel, channel emulators, and UE emulators.

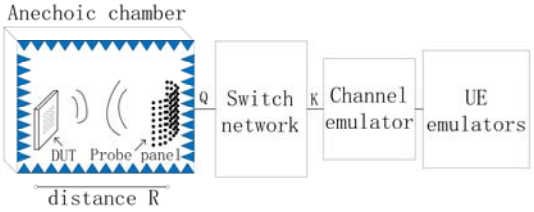


Fig. 2. Illustration of the 3D sectored MPAC OTA setup.

Different from the 2D UE OTA testing, the total variation distance of the PAS [20] is chosen as the evaluation metric to estimate the emulation performance of the PFS and PWS methods in the 3D BS OTA testing. The metric directly evaluates the ability of the two channel emulation methods to reproduce the target PAS under the 3D sectored MPAC setup.

### B. Prerequisite

The spatial correlation is the second moment of the random wave field, which is defined as the statistical similarity between two signals received by two different antennas. For better illustration, we assume vertical polarization throughout this work, while the results can be readily extended to dual-polarized channels. The target spatial correlation can be expressed as:

$$\rho_{Tar} = \int a(\Omega) P(\Omega) a^H(\Omega) d\Omega \,, \tag{1}$$

where $a(\Omega)$ is the steering vector of the antenna array at the solid angle $\Omega$ (which reduces to the azimuth angle in the 2D case), $P(\Omega)$ is the continuous PAS of the target channel, and the superscript $^H$ denotes conjugate transpose. For simplicity, both probes and DUT antennas are assumed to be isotropic. For the PFS method, the corresponding spatial correlation of the MPAC based emulated channel can be expressed as:

$$\rho_{PFS} = \sum_{k=1}^{K} a(\Omega_k) w(\Omega_k) a^H(\Omega_k) \,, \tag{2}$$

where $K$ is the total number of the active probes connected to the channel emulators and $w(\Omega_k)$ is the power weight of the $k$th active probe. The power weights of the $K$ probes can be expressed as a vector $w = [w(\Omega_1), \cdots, w(\Omega_K)]^T$. Then the power weight vector $w$ can be obtained by

solving a convex optimization problem [23]:

$$\begin{aligned} &\arg\min_{w} \left\| \rho_{Tar} - \rho_{PFS}(w) \right\|_2^2 \\ &s.t. \left\| w \right\|_1 = 1, 0 \le w(\Omega_i) \le 1 \left( \forall i \in [1, K] \right) \end{aligned} . \quad (3)$$

For the PWS method, the corresponding spatial correlation of the MPAC based emulated channel can be derived as [19]:

$$\rho_{PWS} = \frac{1}{\beta_0} \sum_{m=1}^{M} \cdot \sum_{k=1}^{K} F(\Omega_k) \omega_{m,k} \sum_{k'=1}^{K} F^H(\Omega_{k'}) \omega_{m,k'}^H , \quad (4)$$

where $M$ is the number of subpaths; $F(\Omega_k)$ is the field patterns of the DUT antennas; $\omega_{m,k}$ is the complex weight of the $k$th active probe for the $m$th subpath:

$$\begin{aligned} \beta_0 = &\sqrt{\sum_{m=1}^{M} \left\| \sum_{k=1}^{K} F(\Omega_k) \omega_{m,k} \right\|^2} \\ &\cdot \sqrt{\sum_{m=1}^{M} \left\| \sum_{k'=1}^{K} F(\Omega_{k'}) \omega_{m,k'} \right\|^2} \end{aligned} , \quad (5)$$

is the normalization factor. In this work, the least square technique is used to calculate the complex weights.

Furthermore, the classic Bartlett beamformer [24] is utilized to estimate the PAS (for it is robust to channel emulation errors):

$$\begin{aligned} U(\Omega) &= a^H(\Omega) \rho_{Tar} a(\Omega) \\ \widehat{U}(\Omega) &= a^H(\Omega) \rho_{OTA} a(\Omega) \end{aligned} , \quad (6)$$

where $U(\Omega)$ and $\widehat{U}(\Omega)$ are the estimated PASs of the target channel and emulation channel, respectively, and $\rho_{OTA}$ represents $\rho_{PFS}$ and $\rho_{PWS}$, respectively. In this work, our main target is to optimize the weights of the OTA probes to reconstruct the spatial channel as close as possible to the target channel, i.e., $\boldsymbol{\rho_{OTA} \approx \rho_{Tar}}$ and $\boldsymbol{\widehat{U}(\Omega) \approx U(\Omega)}$. Moreover, as mentioned before, the total variation distance of the PAS was chosen to evaluate the PAS similarity between the emulated and target channels. This metric reflects the PAS, as well as the size and resolution of the DUT. The Bartlett beamformer and the assumed DUT array are used to estimate the PAS, which is equivalent to observing the power angular distribution of the channel through the limited aperture of the DUT array. The total variation distance of the PAS is calculated as:

$$D_p = \frac{1}{2} \int \left| \frac{\widehat{U}(\Omega)}{\int \widehat{U}(\Omega') d\Omega'} - \frac{U(\Omega)}{\int U(\Omega') d\Omega'} \right| d\Omega , \quad (7)$$

that ranges from 0 (identical) to 1 (complete dissimilar).

## III. SIMULATION AND RESULTS

In the 2D UE OTA testing, the 16 probes are evenly distributed in the horizontal ring. The target channel is set to have two clusters with angle of arrival (AoA) of 0° and 11.25°, respectively. As shown in Fig. 3, when the AoA is set to 0°, there is exactly a probe located at this angle (i.e., the best case), whereas when AoA is set to 11.25°, the incident wave is in between two adjacent probes (i.e., worst case). The angular spreads of arrival (ASA) of each cluster varies from 5° to 35° with 10° steps, and 20 subpaths are generated by each cluster with equal power. The performances of the PFS and PWS methods are evaluated by comparing the similarity of the spatial correlations between the emulated channel and the target channel.

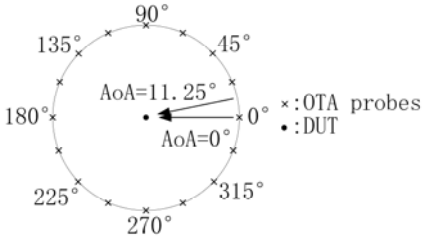


Fig. 3. OTA probe configuration for channel emulation.

The spatial correlations of the target channel and the emulation channel in the two cases are shown in Figs. 4 (a) and (b), respectively. It can be seen that with 16 probes, the test zone size can reach 1.6 λ (where λ is the operation wavelength). In both cases, the PWS method matches the spatial correlation of the target channel well, while the PFS method has poor emulation performance. Nevertheless, with the increase of the ASA, the deviation of the PFS method will gradually decrease, which indicates that the PFS method has poor regeneration ability for clusters with smaller ASA. Furthermore, in the case of large ASA, the spatial correlation of the two methods both well match the target channel, such as 25° and 35°. The results are in accordance with [19]. Therefore, we can speculate that, in the UE testing, the ASA is relatively large due to the abundant scatterers around. As a result, it can be considered that the emulation accuracy of the PFS and PWS methods are roughly the same in this case. However, for the BS testing, the ASA is relatively small because there are not too many scatterers around the BS. Therefore, the PWS method has better emulation performance than its counterpart.

Next, we extend the above analyses to the 3D massive MIMO OTA testing, as shown in Fig. 5. The DUT is assumed to be an 8×8 uniform square array with an inter-element spacing of 0.5 λ. The closest distance between the probe panel and the DUT is set to 2 meters. The probe panel contains 16 evenly distributed probes, and the angular spacing between the probes is 22.5° (which is the same as the 2D case). Figures 5 (a) and (b) correspond to the best case and worst case in the 2D scenario, respectively. Figure 5 (c) shows the four clusters in the best case. Here, the angular spread (AS)

of the elevation and the AS of the azimuth of each cluster are set to 2° and 3°, respectively (corresponding to the CDL-C model [25]).

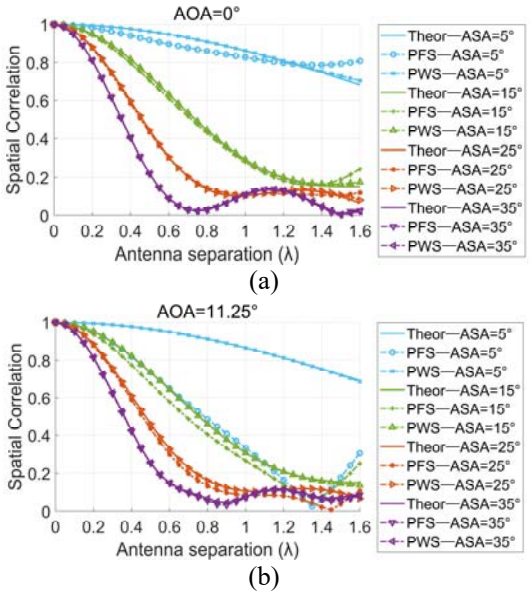


Fig. 4. Spatial correlations of the target and emulated channels when (a) AoA = 0° and (b) AoA = 11.25° (with different ASAs).

The total variation distances of the PAS of the PFS and PWS methods of the three cases (shown in Fig. 5) are listed in Table 1. The results show that, for both the best case and the worst case, the advantage of the PWS is obvious in the case of small AS. Moreover, if the angular spacing between the active probes is large, the increase of cluster will not change the observation that the PWS method is better than the PFS method.

More generally, the sectored MPAC setup is widely used in the 3D massive MIMO OTA testing, as shown in Fig. 2. As mentioned before, the DUT is assumed to be an 8 × 8 uniform square array with an inter-element spacing of 0.5 λ and the shortest distance between the probe panel and the DUT is set to 2 meters. The probe panel contains Q = 629 probes, covering 135° in azimuth and 60° in elevation (with a uniform angular spacing of 3.75°). Furthermore, to consider the influence of the leakage of power spectrum, we add another case where the probe panel contains Q = 1241 probes, covering 270° in azimuth and 60 ° in elevation. Figures 6 (a) and (b) show examples of these two cases with $K$ = 16 active probes. In this work, the 3GPP clustered delay line (CDL) C model [25] has been chosen as the target channel model. Moreover, the spatial angle mapping (SAM) method [20] is taken as the probe selection scheme.

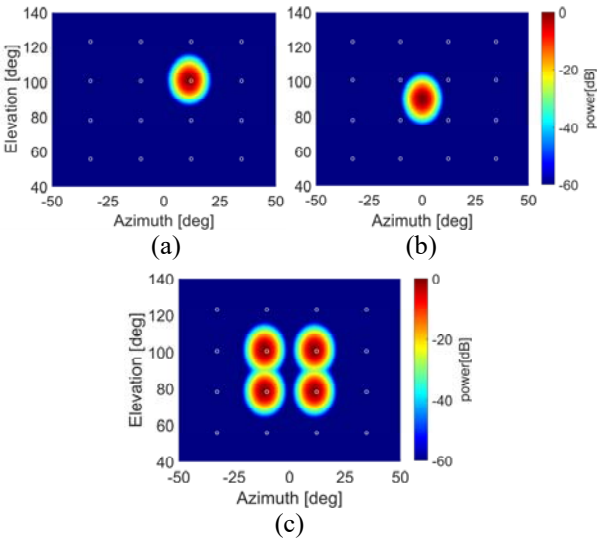


Fig. 5. Illustration of the OTA probe configuration for the PAS of different clusters: (a) the best case; (b) the worst case; (c) four clusters in the best case. White circles represent the active probes.

Table 1: Total variation distances of the PAS of the PFS and PWS methods in the three cases (shown in Fig. 5)

| | **Case 1** | **Case 2** | **Case 3** |
|---|---|---|---|
| PFS | 0.1628 | 0.7590 | 0.1211 |
| PWS | 0.1233 | 0.6826 | 0.0846 |

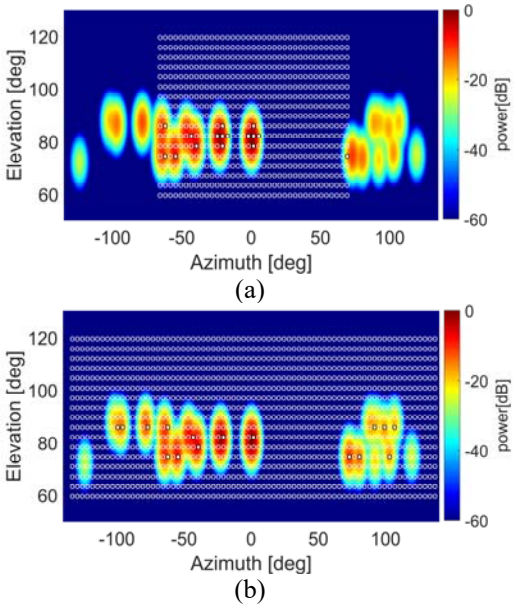


Fig. 6. Illustration of the probe selection for the PAS of the target channel: (a) the general scenario; (b) the full

coverage scenario. White circles represent the available probes and white dots denote the selected active probes.

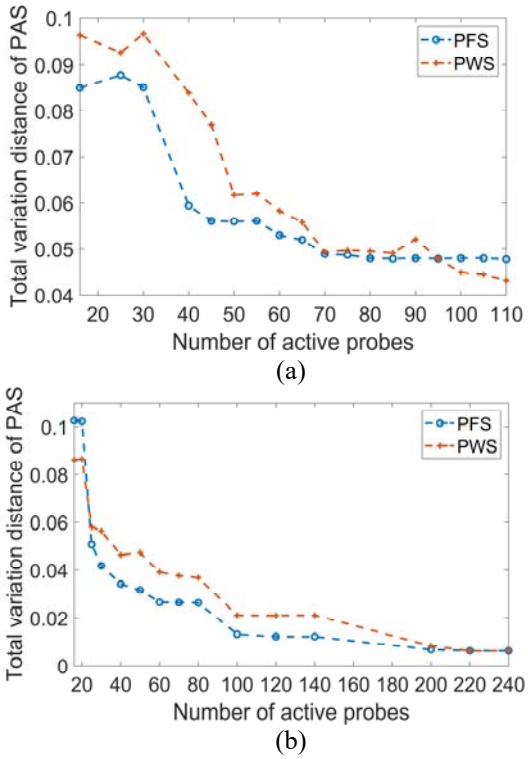


Fig. 7. Deviations of the PAS between PFS and PWS in (a) the general scenario and (b) the full coverage scenario with different number of active probes.

Figure 7 shows the results of the total variation distance of the PAS with different number of active probes of the two scenarios. As can be seen in Fig. 7 (b), when the number of active probes is extremely small (e.g., less than the number of clusters in the probe panel), the PWS method exhibits better performance than the PFS method. This is due to the small AS, which makes up for the disadvantages caused by the number of active probes (it can also be said that the performance of PFS is worse in this case), so that the PWS method has better emulation performance than PFS when the number of probes is particularly small (consistent with the conclusion in Table 1). However, with the increase of the number of active probes (exceeding the number of clusters in the probe panel), as shown in Figs. 7 (a) and (b), the advantages due to the small AS can no longer make up for the disadvantages due to the small number of active probes. Therefore, the PFS method shows better performance than the PWS method. In addition, as the number of active probes continues to increase, the emulation errors of the PFS and PWS methods become smaller, and then the PWS shows better performance.

To further confirm this finding, more simulations are carried out with $K = 629$ and $K = 1241$ active probes of the whole probe panel for the two scenarios. The results show that, in the general scenario, the total variation distance of the PFS is 0.0347, while that of the PWS is 0.0016. In the full coverage scenario, the total variation distance of the PFS is 0.0062, while that of the PWS is 0.00078. Thus, it is safe to conclude that the number of active probes plays a key role in the performance comparisons of the PFS and PWS methods compared with the leakage of the power spectrum. This is easy to understand, since it can be seen from Fig. 6 (a) that the clusters in the probe panel already contain more than 80% of the total power of the target model, so the angle selection of the probe panel in the general scenario is appropriate.

## IV. CONCLUSION

In this paper, we studied the performance of two channel emulation methods in 2D uniform MPAC and 3D sectored MPAC, respectively. It is found that in the case of the traditional 2D MPAC, the PWS method has higher accuracy than the PFS method. In the case of 3D sectored MPAC, however, the results get complicated. It is proved that, compared to the leakage of the power spectrum, the number of active probes plays a more critical role in the performances of the PFS and PWS methods. Furthermore, it can be found that when the number of active probes is less than the number of clusters in the probe panel, the emulation accuracy of the PWS method is better than that of the PFS method. As the number of active probes increases to be greater than the number of clusters in the probe panel, the PFS method then shows better performance than the PWS method. As the number of active probes continues to increase, the deviation of the PFS and PWS methods gradually decrease, and then the PWS method becomes superior to the PFS method.

## ACKNOWLEDGMENT

This work was supported in part by the National Natural Science Foundation of China under Grant 61801366 and the Natural Science Foundation of Shaanxi Province under Grant 2020JM-078, and also supported in part by the Key Research and Development Program of Heilongjiang under Grant GX17A016 and by the Open Project of State Key Laboratory of Millimeter Waves (K2020017).

## REFERENCES

[1] M. Abdullah, Q. Li, W. Xue, G. Peng, Y. He, and X. Chen, "Isolation enhancement of MIMO antennas using shorting pins," *Journal of Electromagnetic Waves and Applications*, vol. 33, no. 10, pp. 1249-1263, July 2018.

[2] A. Zaidi, F. Athley, J. Medbo, U. Gustavsson, G. Durisi, and X. Chen, *5G Physical Layer: Principles, Models and Technology Components*,

Academic Press, 2018.

[3] Y. Li, W. Li, and W. Yu, "A multi-band/UWB MIMO/diversity antenna with an enhanced isolation using radial stub loaded resonator," *Applied Computational Electromagnetics Society Journal*, vol. 28, no. 1, pp. 8-20, Jan. 2013.

[4] F. Faraz, X. Chen, Q. Li, J. Tang, J. Li, T. Khan, and X. Zhang, "Mutual coupling reduction of dual polarized low profile MIMO antenna using decoupling resonators," *Applied Computational Electromagnetics Society Journal*, vol. 35, no. 1, pp. 38-43, Jan. 2020.

[5] K. Yu, Y. Li, and X. Liu, "Mutual coupling reduction of a MIMO antenna array using 3-D novel meta-material structures," *Applied Computational Electromagnetics Society Journal*, vol. 33, no. 7, pp. 758-763, July 2018.

[6] W. Fan, P. Kyösti, Y. Ji, L. Hentilä, X. Chen, and G. F. Pedersen, "Experimental evaluation of user influence on test zone size in multi-probe anechoic chamber setups," *IEEE Access*, vol. 5, pp. 18545-18556, Sep. 2017.

[7] W. Wang, H. Wang, H. Gao, Y. Wu, Y. Liu, and J. Gao, "Plane wave compensation technique for MIMO OTA testing in small multi-probe anechoic chamber," *IET Microwaves Antennas & Propagation*, Apr. 2019.

[8] X. Chen, W. Xue, H. Shi, J. Yi, and W. E. I. Sha, "Orbital angular momentum multiplexing in highly reverberant environments," *IEEE Microw. Wireless Compon. Lett.*, vol. 30, no. 1, pp. 112-115, Jan. 2020.

[9] J. Tang, F. Li, J. Zheng, X. Chen, Y. Li, and J. Chen, "A new mode stirrer design for the reverberation chamber," *Applied Computational Electromagnetics Society Journal*, in press.

[10] W. Yu, Y. Qi, K. Liu, Y. Xu, and J. Fan, "Radiated two-stage method for LTE MIMO user equipment performance evaluation," *IEEE Trans. Electromagn. Compat.*, vol. 56, no. 6, pp. 1691-1696, Dec. 2014.

[11] Y. Jing, H. Kong, and M. Rumney, "MIMO OTA test for a mobile station performance evaluation," *IEEE Instrument. Meas. Mag.*, vol. 19, no. 3, pp. 43-50, June 2016.

[12] CTIA, "Test Plan for 2x2 Downlink MIMO and Transmit Diversity Over-the-Air Performance," Tech. Rep. Version 1.1.1, Sep. 2017.

[13] W. Fan, X. Carreno, P. Kyosti, J. O. Nielsen, and G. F. Pedersen, "Over-the-air testing of MIMO-capable terminals: Evaluation of multiple-antenna systems in realistic multipath propagation environments using an OTA method," *IEEE Veh. Technol. Mag.*, vol. 10, no. 2, pp. 38-46, June 2015.

[14] X. Chen, W. Fan, L. Hentilä, P. Kyösti, and G. F. Pedersen, "Throughput modeling and validations for MIMO-OTA testing with arbitrary multipath," *IEEE Antennas Wireless Propag. Lett.*, vol. 17, no. 4, pp. 637-640, Apr. 2018.

[15] R. He, B. Ai, G. Wang, M. Yang, C. Huang, and Z. Zhong, "Wireless channel sparsity: Measurement, analysis, and exploitation in estimation," *IEEE Wireless Communications*, in press.

[16] F. Zhang, W. Fan, Y. Ji, M. Gustafsson, T. Jamsa, G. Steinböck, P. Kyösti, and G. F. Pedersen, "Performance testing of massive MIMO base station with multi-probe anechoic setups," *Proc. 12th Eur. Conf. Antennas Propag. (EUCAP)*, pp. 1-5, Apr. 2018.

[17] A. Khatun, V. M. Kolmonen, V. Hovinen, D. Parveg, M. Berg, K. Haneda, K. Nikoskinen, and E. Salonen, "Experimental verification of a plane-wave field synthesis technique for MIMO OTA antenna testing," *IEEE Trans. Antennas Propag.*, vol. 64, no. 7, pp. 3141-3150, July 2016.

[18] P. Kyösti, T. Jämsä, and J.-P. Nuutinen, "Channel modelling for multiprobe over-the-air MIMO testing," *International Journal of Antennas and Propagation*, vol. 2012, Mar. 2012.

[19] Y. Ji, W. Fan, G. F. Pedersen, and X. Wu, "On channel emulation methods in multiprobe anechoic chamber setups for over-the-air testing," *IEEE Trans. Veh. Technol.*, vol. 67, no. 8, pp. 6740-6751, Aug. 2018.

[20] W. Fan, P. Kyösti, M. Romney, X. Chen, and G. F. Pedersen, "Over-the-air radiated testing of millimeter-wave beam-steerable devices in a cost-effective measurement setup," *IEEE Commun. Mag.*, vol. 56, no. 7, pp. 64-71, July 2018.

[21] H. Pei, X. Chen, W. Fan, M. Zhang, A. Zhang, and T. Svensson, "Comparisons of channel emulation methods for state-of-the-art multi-probe anechoic chamber based millimeter-wave over-the-air testing," *IEEE VTC-Fall*, Honolulu, HI, Sep. 2019.

[22] Y. Li, L. Xin, and X. Zhang, "On probe weighting for massive MIMO OTA testing based on angular spectrum similarity," *IEEE Antennas and Wireless Propagation Letters*, vol. 18, pp. 1497-1501, July 2019.

[23] S. Boyd and L. Vandenberghe, *Convex Optimization*. Cambridge University Press, Mar. 2004.

[24] P. Stoica and R. L. Moses, *Spectral Analysis of Signals*. Pearson/Prentice Hall Upper Saddle River, NJ, 2005.

[25] TR 38.901, "Study on channel model for frequencies from 0.5 to 100 GHz," 3GPP, Tech. Rep. V14.1.1, July 2017.